

# Hole spin polarization in GaAlAs:Mn structures

A. Ghazali

*Groupe de Physique des Solides,  
UMR 7588-CNRS, Universités Paris 7  
et Paris 6*

*Tour 23, 2 Place Jussieu, F-75 251 Paris Cedex 05, France*

I. C. da Cunha Lima, and M. A. Boselli

*Instituto de Física, Universidade do Estado do Rio de Janeiro  
Rua São Francisco Xavier 524, 20.500-013 Rio de Janeiro, R.J., Brazil*

A self-consistent calculation of the electronic properties of GaAlAs:Mn magnetic semiconductor quantum well structures is performed including the Hartree term and the  $sp-d$  exchange interaction with the Mn magnetic moments. The spin polarization density is obtained for several structure configurations. Available experimental results are compared with theory.

During the last years spin-polarized transport became a matter of major interest<sup>1,2</sup>, giving rise to a field usually called magnetoelectronics, or spintronics. Much effort has been made in studying and producing the so-called spin-valve, where a spin-polarized current is generated. A promising system in that area is the recently grown structure of GaAs/AlAs with inclusions of  $\text{Ga}_{1-x}\text{Mn}_x\text{As}$  layers<sup>3-9</sup>. Homogeneous samples of  $\text{Ga}_{1-x}\text{Mn}_x\text{As}$  alloys with  $x$  up to 7% have been produced, avoiding the formation of MnAs clusters by using low temperature (200 – 300° C) MBE techniques. In  $\text{Ga}_{1-x}\text{Mn}_x\text{As}$ , a new prototype of Diluted Magnetic Semiconductors (DMS)<sup>10,11</sup>, the  $\text{Mn}^{2+}$  cations have the  $3d$  shell partially filled with five electrons, in such a way that they carry a magnetic moment of  $S = 5/2$ . In addition, the Mn ion binds a hole to satisfy charge neutrality. Besides its practical importance, this kind of DMS introduces an interesting problem from the physical point of view: Mn in the alloy is a strong  $p$  dopant, the free hole concentration reaching even  $p = 10^{20-21}\text{cm}^{-3}$ . At small Mn concentrations, the alloy is a paramagnetic insulator. As  $x$  increases it becomes ferromagnetic, going through a non-metal/metal transition for higher concentrations ( $x \approx 0.03$ ), and keeping its ferromagnetic phase. For  $x$  above 5%, the alloy becomes a ferromagnetic insulator. In the metallic phase, the ferromagnetic transition is observed in the range of 30 – 100K, depending on the value of  $x$ , among the highest transitions temperatures observed in DMS. The  $sp-d$  exchange interaction of Ruderman-Kittel-Kasuya-Yosida (RKKY) type has been recognized as the main origin of the observed ferromagnetism in the metallic phase of III-V based DMSs<sup>7</sup>.

A few years ago Helman and Baltensperger<sup>12,13</sup> performed analytical RKKY calculations for the spin polar-

ization in several confined structures, and clarified the role of the confined states in the multilayer interaction. Recently, improvements on the standard RKKY mechanism were introduced by Byounggak Lee *et al*<sup>14</sup> to treat the ferromagnetism of GaMnAs quantum wells. In the present work we consider a  $\text{Ga}_{1-x}\text{Mn}_x\text{As}$  layer in its metallic phase, grown inside a GaAs/AlAs quantum well structure. We obtain the spin-polarized electronic structure for holes, taking into account their interaction with the magnetic impurities. The Hamiltonian we consider is:

$$H = H_0 + U_H + U_{mag}, \quad (1)$$

$$U_{mag}(\vec{r}) = -I \sum_{i=1}^{N_i} \vec{s}(\vec{r}) \cdot \vec{S}(\vec{R}_i) \delta(\vec{r} - \vec{R}_i). \quad (2)$$

The  $H_0$  term in the rhs of Eq. (1) contains the kinetic energy and the confining potential,  $U_c(z)$ , due to the band edges mismatch at the semiconductor interfaces. Coulomb interactions between carriers are considered through the Hartree term  $U_H(\vec{r})$ . The hole system is supposed to be homogeneous in the  $xy$  plane, so  $U_H(\vec{r}) = U_H(z)$ . In the present approach we treat the magnetic interaction as being due to an uniform magnetization in the DMS. If a net magnetization exists, it will polarize the hole gas. This problem is solved self-consistently by a secular matrix equation in the reciprocal space. The method would be exact were not for cutting the matrix size. The advantage is that it provides spin-polarized eigenvalues and eigenfunctions with high accuracy, not only for bound states, but also for a high number of scattering states. For each spin, we define the wavefunction Fourier Transform (FT):

$$\psi_\sigma(\vec{r}) = \int d^3q \exp(i\vec{q}\cdot\vec{r}) \psi_\sigma(\vec{q}). \quad (3)$$

The hole eigenstates will be obtained by discretizing the integrals on  $\vec{q}$  appearing in

$$\int d^3r \psi_\sigma^*(\vec{r}) (H - E) \psi_\sigma(\vec{r}) = 0. \quad (4)$$

When integrating the magnetic term in the Hamiltonian over  $\vec{r}$ , we assumed the magnetic impurities to be uniformly distributed in the  $\text{Ga}_{1-x}\text{Mn}_x\text{As}$  DMS layer, all of

them having the same magnetization, namely the thermal average magnetization  $\langle \vec{M} \rangle$ . This treatment includes not only the ferromagnetic phase but also phases where a partial magnetization is observed, the ‘‘canted-spin’’ phases<sup>15,16</sup>. Therefore,

$$\begin{aligned}
& -I \int d^3r \exp[i(\vec{q} - \vec{q}') \cdot \vec{r}] \sum_{i=1}^{N_i} \vec{s}(\vec{r}) \cdot \vec{S}(\vec{R}_i) \delta(\vec{r} - \vec{R}_i) \simeq \\
& -I \frac{\sigma}{2} \langle M \rangle \sum_{i=1}^{N_i} \exp[i(\vec{q} - \vec{q}') \cdot \vec{R}_i] = \\
& -I \frac{\sigma}{2} \langle M \rangle \frac{N_i}{V} \int d^3R_i \exp[i(\vec{q} - \vec{q}') \cdot \vec{R}_i] = \\
& -\tilde{I} \frac{\sigma}{2} x \langle M \rangle F_{DMS}(q_z - q'_z) (2\pi)^3 \delta^2(\vec{q}_{\parallel} - \vec{q}'_{\parallel}), \quad (5)
\end{aligned}$$

where  $\frac{N_i}{V}$  is the impurity density, and  $\sigma = \pm 1$  for spin parallel (upper sign) or anti-parallel (lower sign) to the magnetization.  $F_{DMS}$  is the integral performed on the  $z$ -coordinate along the DMS layer:

$$F_{DMS}(q) \equiv \frac{1}{2\pi} \int_{DMS} dz \exp[iq \cdot z]. \quad (6)$$

In Eq.(5) we have defined  $\tilde{I} = \frac{I}{v_0}$ , where  $v_0$  is the volume of the  $\text{Mn}^{2+}$  ion, which is the  $fcc$  lattice’s primitive cell volume,  $a^3/4$ . It is worthwhile to mention that, in experimental works,  $\tilde{I}$  is usually represented by  $N_0\beta$ . Here we used  $N_0\beta = -1.2\text{eV}^{18}$ . After performing the FT of the Hartree term plus the confining potential,

$$U_{el}(q) = \frac{1}{2\pi} \int dz \exp[iq \cdot z] [U_H(z) + U_c(z)], \quad (7)$$

the eigenvalues and eigenfunctions at the bottom of the 2-D subbands may be obtained by solving the secular matrix for each spin-polarization:

$$\det \left\{ \left[ \frac{\hbar^2 q_z^2}{2m^*} - E \right] \delta(q_z - q'_z) + U_{el}(q_z - q'_z) - \tilde{I} \frac{\sigma}{2} \langle M \rangle F_{DMS}(q_z - q'_z) \right\} = 0. \quad (8)$$

For applications, favorable spin configurations may be designed by growing a proper structure. In particular, the possibility of having a ferromagnetic order in the DMS heterostructures is important for spin tunneling and resonant spin tunneling in nanostructures<sup>8,19</sup>. We have calculated the electronic structure, and the spin polarization, in three GaAlAs/GaAs:Mn quantum wells. We started with an AlAs/GaAs QW in the middle of which a DMS barrier ( $\text{Ga}_{0.65-x}\text{Al}_{0.35}\text{Mn}_x\text{As}$ ) is grown in its ferromagnetic metallic phase. In that case, we have, actually, two QW of widths  $L$  separated by an internal barrier of 168.3 meV with thickness  $d$ , and barriers of 529 meV at the lateral boundaries. In a second structure, we assume that the DMS is just a  $\text{Ga}_{1-x}\text{Mn}_x\text{As}$  layer of thickness  $d$ , no internal barrier being structurally

imposed. Finally, in a last structure, we explore the case of a single DMS QW: a  $\text{Ga}_{1-x}\text{Mn}_x\text{As}$  layer of thickness  $2L + d$  is surrounded by thick layers of AlAs. It is well known that in ferromagnetic metallic  $\text{Ga}_{1-x}\text{Mn}_x\text{As}$  layers (in our calculation we assumed  $x = 0.05$ ) the density of free carriers (holes) is just a fraction of the density of the magnetic ions. Throughout the present calculation we made the hole density  $p = 1. \times 10^{20} \text{cm}^{-3}$ ,  $T=0\text{K}$ , and  $\langle M \rangle = 5/2$ . Due to the high carrier density, the Hartree term cannot be neglected, and several subbands happen to be occupied.

The results for the energy of the bound states are shown in Table I, the arrows indicating spin up or down, i.e., parallel or anti-parallel to the DMS magnetization. For the first two structures  $L = 50$  nm, and  $d = 1$  nm. The criteria for self-consistency has been chosen to be a ratio  $(E_F(i) - E_F(i-1))/2(E_F(i) + E_F(i-1)) < .00001$ , where  $E_F(i)$  is the calculated Fermi energy exiting iteration  $i$ .

The charge density distributions are shown in Fig. 1 for samples #1 and #2. In the case of the first sample we observe a dip at the middle of the structure, as a consequence of the existence of the central barrier. A much less pronounced dip is observed in the sample #1’s spin polarization density, shown in Fig. 2. By integrating the spin density we obtain that 6% of the spins are polarized.

TABLE I. Energies (in eV) of the bound states, reckoned from the top of the AlAs valence band edge. Arrows represent the spin polarization of the state, up for parallel, down for anti-parallel to the average  $\text{Mn}^{2+}$  magnetization.

state	sample 1	spin	sample 2	spin	sample 3	spin
1	-0.51819	↓	-0.54815	↓	-0.59511	↓
2	-0.51398	↑	-0.51799	↑	-0.58266	↓
3	-0.51244	↓	-0.51233	↓	-0.56052	↓
4	-0.51199	↑	-0.51167	↑	-0.52939	↓
5	-0.47744	↓	-0.49945	↓	-0.48941	↓
6	-0.46498	↑	-0.47861	↑	-0.44520	↑
7	-0.45885	↓	-0.46045	↓	-0.44070	↓
8	-0.45722	↑	-0.45806	↑	-0.43300	↑
9	-0.40581	↓	-0.42870	↓	-0.41125	↑
10	-0.38491	↑	-0.40766	↑	-0.38341	↓
11	-0.36957	↓	-0.37390	↓	-0.38069	↑
12	-0.36612	↑	-0.36903	↑	-0.34152	↑
13	-0.30218	↓	-0.32280	↓	-0.31775	↓
14	-0.27688	↑	-0.30397	↑	-0.29390	↑
15	-0.24647	↓	-0.25385	↓	-0.24409	↓
16	-0.24076	↑	-0.24624	↑	-0.23809	↑
17	-0.16722	↓	-0.18438	↓	-0.17455	↑
18	-0.14316	↑	-0.16859	↑	-0.16311	↓
19	-0.09378	↓	-0.10369	↓	-0.10420	↑
20	-0.08594	↑	-0.09386	↑	-0.07647	↓
21	-0.01095	↓	-0.02272	↓	-0.03001	↑
22	-	-	-0.01170	↑	-	-
$E_F$	-0.49486	-	-0.50324	-	-0.40430	-

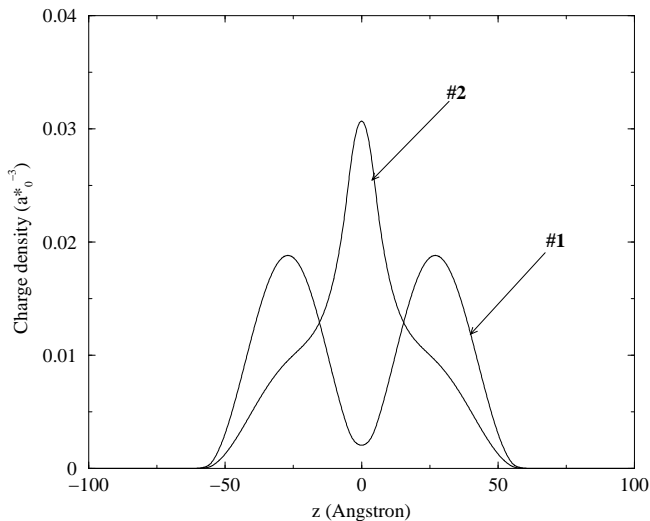


FIG. 1. Charge density as a function of the distance to the center of the well. Sample #1: two GaAs quantum wells of 50Å separated by a 10Å barrier of  $\text{Ga}_{0.60}\text{Al}_{0.35}\text{Mn}_{0.05}$ . Sample #2: a 10Å  $\text{Ga}_{0.95}\text{Mn}_{0.05}\text{As}$  instead of the middle barrier.

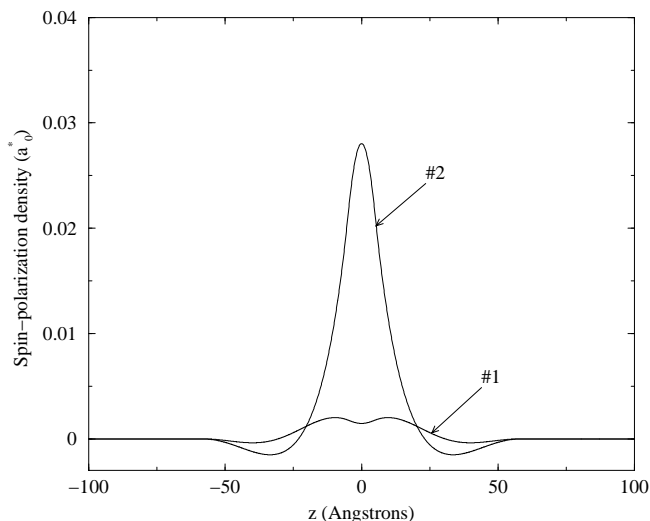


FIG. 2. Spin polarization density as a function of the distance to the center of the well, for samples #1 and #2.

The elimination of the central barrier in sample #2 increases the probability of finding the holes in the middle of the structure, now attracted by the unbalanced negative charges. The dip disappears giving rise to a pronounced peak in both the charge density and the spin polarization density. Another important difference is the Friedel-like oscillation in the polarization, being anti-parallel in the middle of the well, and parallel near the interfaces. The total polarization reaches 40%.

A radical change occurs when the DMS occupies the entire well, as shown in Fig. 3. The number of carriers per unit area is much greater than in the previous cases, and many subbands are occupied. The charge density shows an oscillation inside the well, as a consequence of

the higher subbands occupation. The oscillations that occurs in the spin polarization density follow those in the charge density. In the case where charges and magnetic moments cohabit inside a finite width determined by the quantum confinement, we obtain that the oscillations are not enough to invert the polarization in any region. We plotted the sum of the bare confining potential plus the self-consistent Hartree term in the inset of Fig. 3. An effective central barrier appears at the middle of the well, together with two valleys at the interfaces what increases the lateral barriers from 529 meV to about 600 meV. In sample #3 the magnetic interaction between holes and the ferromagnetic layer contributes to the confining potential with an increase of 150 meV for spin anti-parallel, and a decrease of the same amount for spin parallel. Therefore, there is no rigid shift of the eigenenergies as in a 3-D system. The total polarization is 82%.

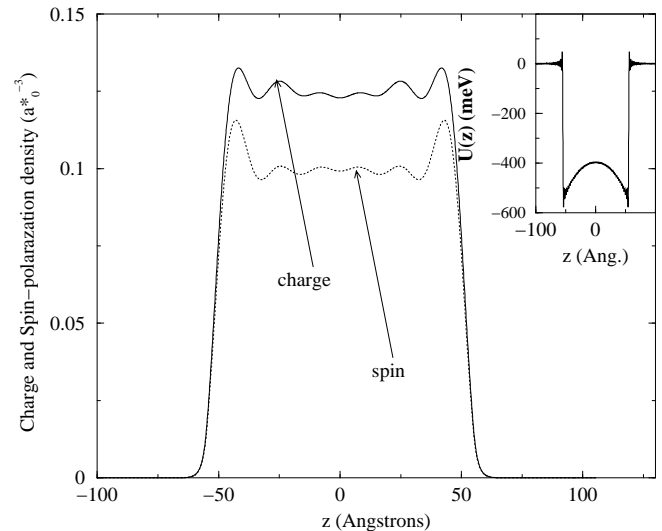


FIG. 3. Sample #3: Charge density and spin density distributions in a single quantum well of 110Å  $\text{Ga}_{0.95}\text{Mn}_{0.05}\text{As}$ . Inset: bare confining potential plus self-consistent Hartree term.

The spin-polarized electronic structure in diluted magnetic semiconductors, as obtained here, points to the possibility of a self-consistent calculation of the magnetization in multilayered structures, as in Refs. 15 and 16, taking into account a spin-polarized RKKY mechanism. Recently Chiba *et al*<sup>17</sup> investigated a GaMnAs trilayer structure and observed a ferromagnetic, although weak, interaction between two ferromagnetic layers. The present result is also important for determining properties like spin diffusion and spin filtering in cases where spin-coherence lifetimes are large. For instance, the spin motion for carriers polarized parallel and anti-parallel to the equilibrium polarization in otherwise non-magnetic GaAs samples has been predicted<sup>20</sup> to show a difference of an order of magnitude between the two speeds, with electrons and holes behaving in opposite way. This fact points to the importance of taking a properly calculated

electronic structure in obtaining the spin-polarized transport in magnetic GaMnAs structures. On the other hand, a spin filtering mechanism has been previewed in the ZnSe/ZnMnSe/ZnSe structure with an external applied magnetic field<sup>21</sup>. The present results on the electronic structure of GaMnAs shows the possibility of filtering spins without needing an external field in the range of temperatures of ferromagnetic phases.

### ACKNOWLEDGMENTS

This work was partially supported by CAPES, FAPERJ and CENAPAD/UNICAMP-FINEP in Brazil, and by the PAST grant from Ministère de l'Éducation Nationale, de l'Enseignement Supérieur et de la Recherche (France).

- <sup>14</sup> Byoung-hak Lee, T. Jungwirth, and A. H. MacDonald, Phys. Rev. B **61**, 15 606 (2000).  
<sup>15</sup> M. A. Boselli, I. C. da Cunha Lima, and A. Ghazali, J. Appl. Phys. **87**, 6439 (2000).  
<sup>16</sup> M. A. Boselli, A. Ghazali, and I. C. da Cunha Lima, Phys. Rev. B **62**, No 13 (2000), under press.  
<sup>17</sup> D. Chiba, N. Akiba, F. Matsukura, Y. Ohno, and H. Ohno, Appl. Phys. Lett. **77**, 1873 (2000).  
<sup>18</sup> J. Okabayashi, A. Kimura, O. Rader, T. Mizokawa, A. Fujimori, T. Hayashi, and M. Tanaka, Phys. Rev. B **58**, R4211 (1998).  
<sup>19</sup> P. Bruno and C. Chappert, Phys. Rev. Lett. **67**, 1602 (1991).  
<sup>20</sup> Michael E. Flatté and Jeff M. Byers, Phys. Rev. Lett. **84**, 4220 (2000).  
<sup>21</sup> J. C. Egues, Phys. Rev. Lett. **80**, 4578 (1998).

- 
- <sup>1</sup> R. Fiederling, M. Keim, G. Reuscher, W. Ossau, G. Schmidt, A. Waag and L. W. Molenkamp, Nature **402**, 787 (1999).  
<sup>2</sup> Y. Ohno, D. K. Young, B. Beschoten, F. Matsukura, H. Ohno and D. D. Awschalom, Nature **402**, 790 (1999).  
<sup>3</sup> A. Van Esch, L. van Bockstal, J. De Boeck, G. Verbank, A.S. van Steenbergen, P.J. Wellmann, B. Grietens, R. Bogaerts, F. Herlach, and G. Borghs, Phys. Rev. B **56**, 13103 (1997).  
<sup>4</sup> A. Van Esch, J. De Boeck, L. Van Bockstal, R. Bogaerts, F. Herlach, and G. Borghs, J. Phys.: Condens. Matter **9**, L361 (1997).  
<sup>5</sup> A. Oiwa, S. Katsumoto, A. Endo, M. Hirasawa, Y. Iye, H. Ohno, F. Matsukura, A. Shen, and Y. Sugawara, Solid State Commun. **103**, 209 (1997).  
<sup>6</sup> A. Shen, H. Ohno, F. Matsukura, Y. Sugawara, N. Akiba, T. Kuroiwa, A. Oiwa, A. Endo, S. Katsumoto, Y. Iye, J. Crys. Growth **175/176**, 1069 (1997).  
<sup>7</sup> F. Matsukura, H. Ohno, A. Shen, and Y. Sugawara, Phys. Rev. B **57**, R2037 (1998).  
<sup>8</sup> H. Ohno, N. Akiba, F. Matsukura, A. Shen, K. Ohtani, Y. Ohno, Appl. Phys. Lett. **73**, 363 (1998).  
<sup>9</sup> H. Ohno, F. Matsukura, T. Omiya, and N. Akida, J. Appl. Phys. **85**, 4277 (1999).  
<sup>10</sup> J.K. Furdyna and J. Kossut, in *Diluted Magnetic Semiconductors*, edited by J.K. Furdyna and J. Kossut, Semiconductors and Semimetals, Vol. 24, edited by R.K. Willardson and A.C. Beer (Academic Press, N.Y., 1988).  
<sup>11</sup> T. Dietl, in *(Diluted) Magnetic Semiconductors*, edited by T.S. Moss, Handbook of Semiconductors, Vol. 3, edited by S. Mahajan (Elsevier Science B.V., 1994).  
<sup>12</sup> J.S. Helman and W. Baltensperger, Phys. Rev. B **50**, 12682 (1994).  
<sup>13</sup> J.S. Helman and W. Baltensperger, Phys. Rev. B **53**, 275 (1996).